

# A generalized multiscale finite element method for neutron transport problems in $SP_3$ approximation

Aleksandr O. Vasilev<sup>a,\*</sup>, Denis A. Spiridonov<sup>a</sup>, Alexander V. Avvakumov<sup>b</sup>

<sup>a</sup>*North-Eastern Federal University, 58, Belinskogo, Yakutsk, Russia*

<sup>b</sup>*National Research Center Kurchatov Institute, 1, Sq. Academician Kurchatov, Moscow, Russia*

---

## Abstract

The  $SP_3$  approximation of the neutron transport equation allows improving the accuracy for both static and transient simulations for reactor core analysis compared with the neutron diffusion theory. Besides, the  $SP_3$  calculation costs are much less than higher order transport methods ( $S_N$  or  $P_N$ ). Another advantage of the  $SP_3$  approximation is a similar structure of equations that is used in the diffusion method. Therefore, there is no difficulty to implement the  $SP_3$  solution option to the multi-group neutron diffusion codes.

In this paper, we attempt to employ a model reduction technique based on the multiscale method for neutron transport equation in  $SP_3$  approximation. The proposed method is based on the use of a generalized multiscale finite element method (GMsFEM). The main idea is to create multiscale basis functions that can be used to effectively solve on a coarse grid. From calculation results, we obtain that multiscale basis functions can properly take into account the small-scale characteristics of the medium and provide accurate solutions. The application of the  $SP_3$  methodology based on solution of the  $\lambda$ -spectral problems has been tested for the some reactor benchmarks. The results calculated with the GMsFEM are compared with the reference transport calculation results.

*Keywords:* neutron transport equation,  $SP_3$  approximation, eigenvalues, multiscale simulation, generalized multiscale finite element method (GMsFEM)

---

## 1. Introduction

## 2. Problem statement

Let's consider the symmetric form of the  $SP_3$  equation for the neutron flux (?). The neutron dynamics is considered in the limited convex two-dimensional

---

\*Corresponding author

Email addresses: [haska87@gmail.com](mailto:haska87@gmail.com) (Aleksandr O. Vasilev), [d.stalnov@mail.ru](mailto:d.stalnov@mail.ru) (Denis A. Spiridonov), [Avvakumov2009@rambler.ru](mailto:Avvakumov2009@rambler.ru) (Alexander V. Avvakumov)

or three-dimensional area  $\Omega$  ( $\mathbf{x} = \{x_1, \dots, x_d\} \in \Omega$ ,  $d = 2, 3$ ) with boundary  $\partial\Omega$ . The neutron transport is described by the system of equations

$$\begin{aligned} \frac{1}{v_g} \frac{\partial \phi_{0,g}}{\partial t} - \frac{2}{v_g} \frac{\partial \phi_{2,g}}{\partial t} - \nabla \cdot D_{0,g} \nabla \phi_{0,g} + \Sigma_{r,g} \phi_{0,g} - 2\Sigma_{r,g} \phi_{2,g} = \\ = (1 - \beta) \chi_{n,g} S_n + S_{s,g} + \chi_{d,g} S_d, \\ - \frac{2}{v_g} \frac{\partial \phi_{0,g}}{\partial t} + \frac{9}{v_g} \frac{\partial \phi_{2,g}}{\partial t} - \nabla \cdot D_{2,g} \nabla \phi_{2,g} + (5\Sigma_{t,g} + 4\Sigma_{r,g}) \phi_{2,g} - 2\Sigma_{r,g} \phi_{0,g} = \\ = -2(1 - \beta) \chi_{n,g} S_n - 2S_{s,g} - 2\chi_{d,g} S_d, \end{aligned} \quad (1)$$

where

$$\begin{aligned} S_n = \sum_{g'=1}^G \nu \Sigma_{f,g'} \phi_{g'}, \quad S_{s,g} = \sum_{g \neq g'=1}^G \Sigma_{s,g' \rightarrow g} \phi_{g'}, \quad S_d = \sum_{m=1}^M \lambda_m c_m, \\ \phi_{0,g} = \phi_g + 2\phi_{2,g}, \quad D_{0,g} = \frac{1}{3\Sigma_{tr,g}}, \quad D_{2,g} = \frac{9}{7\Sigma_{t,g}}, \quad g = 1, 2, \dots, G. \end{aligned}$$

Here  $G$  — number of energy groups,  $\phi_g(\mathbf{x}, t)$  — scalar flux,  $\phi_{0,g}(\mathbf{x}, t)$  — pseudo 0th moment of angular flux,  $\phi_{2,g}(\mathbf{x}, t)$  — second moment of angular flux,  $\Sigma_{t,g}(\mathbf{x}, t)$  — total cross-section,  $\Sigma_{tr,g}(\mathbf{x}, t)$  — transport cross-section,  $\Sigma_{r,g}(\mathbf{x}, t)$  — removal cross-section,  $\Sigma_{s,g' \rightarrow g}(\mathbf{x}, t)$  — scattering cross-section,  $\chi_g$  — spectra of neutrons,  $\nu \Sigma_{f,g}(\mathbf{x}, t)$  — generation cross-section,  $c_m(\mathbf{x}, t)$  — density of sources of delayed neutrons,  $\lambda_m$  — decay constant of sources of delayed neutrons,  $M$  — number of types of delayed neutrons.

The density of sources of delayed neutrons is described by the equations

$$\frac{\partial c_m}{\partial t} + \lambda_m c_m = \beta_m S_n, \quad m = 1, 2, \dots, M, \quad (2)$$

where  $\beta_m$  is the fraction of delayed neutrons of m-type, and

$$\beta = \sum_{m=1}^M \beta_m.$$

The Marshak-type conditions are set at the boundary of the area  $\partial\Omega$

$$\begin{bmatrix} J_{0,g}(\mathbf{x}) \\ J_{2,g}(\mathbf{x}) \end{bmatrix} = \begin{bmatrix} \frac{1}{2} & -\frac{3}{8} \\ \frac{3}{8} & \frac{21}{8} \end{bmatrix} \begin{bmatrix} \phi_{0,g}(\mathbf{x}) \\ \phi_{2,g}(\mathbf{x}) \end{bmatrix}, \quad J_{i,g}(\mathbf{x}) = -D_{i,g} \nabla \phi_{i,g}(\mathbf{x}), \quad i = 0, 2. \quad (3)$$

System of equations (1) and (2) is supplemented with boundary conditions (3) and corresponding initial conditions

$$\phi_g(\mathbf{x}, 0) = \phi_g^0(\mathbf{x}), \quad g = 1, 2, \dots, G, \quad c_m(\mathbf{x}, 0) = c_m^0(\mathbf{x}), \quad m = 1, 2, \dots, M. \quad (4)$$

We assume that at the initial time  $t = 0$ , the reactor is in steady-state critical condition.

**Discretization.** Define a uniform grid

$$\omega = \{t^n = n\tau, \quad n = 0, 1, \dots, N, \quad \tau N = T\}$$

and use the next notations  $\phi_g^n = \phi_g(\mathbf{x}, t^n)$ ,  $c_m^n = c_m(\mathbf{x}, t^n)$ . We discretize the time derivatives of equation (1) using finite-difference scheme. For approximation in time, we use a fully implicit scheme with time step  $\tau$ . For delayed neutron source equation we use numerical-analytical method for the construction of approximations in time. The equation (2) in the equivalent form

$$\frac{\partial e^{\lambda_m t} c_m}{\partial t} = \beta_m e^{\lambda_m t} \sum_{g=1}^G \nu \Sigma_{fg} \phi_g, \quad m = 1, 2, \dots, M.$$

After integration on time interval  $[t^n, t^{n+1}]$  one can obtain

$$c_m^{n+1} = e^{-\lambda_m \tau} c_m^n + \beta_m \int_{t^n}^{t^{n+1}} e^{\lambda_m(t-t^{n+1})} \sum_{g=1}^G \nu \Sigma_{fg} \phi_g dt, \quad m = 1, 2, \dots, M. \quad (5)$$

For spatial approximation we use the finite element method. Let  $H^1(\Omega)$  – Sobolev space,  $q \in H^1$ :  $q^2$  and  $|\nabla q|^2$  have a finite integral in  $\Omega$ . Using the integration by parts, we obtain the following variational formulation: let's find  $\phi_g^{n+1} \in V^G$  such that

$$\begin{aligned} & \int_{\Omega} \left( \frac{\phi_{0,g}^{n+1} - \phi_{0,g}^n}{v_g \tau} - \frac{2(\phi_{2,g}^{n+1} - \phi_{2,g}^n)}{v_g \tau} \right) q_g d\mathbf{x} - \int_{\Omega} D_{0,g} \nabla \phi_{0,g}^{n+1} \nabla q_g d\mathbf{x} + \int_{\partial\Omega} J_{0,g} q_g d\mathbf{s} + \\ & \int_{\Omega} (\Sigma_{r,g} \phi_{0,g}^{n+1} - 2\Sigma_{r,g} \phi_{2,g}^{n+1}) q_g d\mathbf{x} = \int_{\Omega} ((1-\beta)\chi_{n,g} S_n + S_{s,g} + \chi_{d,g} S_d) q_g d\mathbf{x}, \\ & \int_{\Omega} \left( -\frac{2(\phi_{0,g}^{n+1} - \phi_{0,g}^n)}{v_g \tau} + \frac{9(\phi_{2,g}^{n+1} - \phi_{2,g}^n)}{v_g \tau} \right) q_g d\mathbf{x} - \int_{\Omega} D_{2,g} \nabla \phi_{2,g}^{n+1} \nabla q_g d\mathbf{x} + \int_{\partial\Omega} J_{2,g} q_g d\mathbf{s} + \\ & \int_{\Omega} ((5\Sigma_{t,g} + 4\Sigma_{r,g})\phi_{2,g}^{n+1} - 2\Sigma_{r,g}\phi_{0,g}^{n+1}) q_g d\mathbf{x} = \int_{\Omega} (-2(1-\beta)\chi_{n,g} S_n - 2S_{s,g} - 2\chi_{d,g} S_d) q_g d\mathbf{x}, \end{aligned} \quad (6)$$

where  $V^G = [H^1(\Omega)]^G$ .

Further, it's necessary to pass from the continuous variational problem (6) to the discrete problem. We introduce finite-dimensional space of finite elements  $V_h^G \subset V^G$  and formulate a discrete variational problem. We use standard linear basis functions as basis functions to solve the problem on the fine grid. The problem is solving a system of linear algebraic equations

$$A_f \phi = b_f, \quad (7)$$

where the operator  $A_f$  corresponds to the left side of equation, and the vector  $b_f$  corresponds to the right side of equation (6).

### 3. Multiscale method

For the discretization on the coarse grid we use GMsFEM. We construct two grids: fine grid ( $\mathcal{T}_h$ ) and coarse grid ( $\mathcal{T}_H$ ) (see Figure 1). For multiscale basis construction, we define local domains  $\omega_i$ , where  $i = 1, \dots, N_v$  and  $N_v$  is the number of coarse grid nodes. We assume that  $\mathcal{T}_h$  is a refinement of  $\mathcal{T}_H$ , where  $h$  and  $H$  represent the fine and coarse grid sizes, respectively. We assume that the fine-scale grid  $\mathcal{T}_h$  is sufficiently fine to fully resolve the small-scale information of the domain while  $\mathcal{T}_H$  is a coarse grid containing many fine-scale features. A local domain  $\omega_i$  is obtained by the combining all the coarse cells around one vertex of the coarse grid.

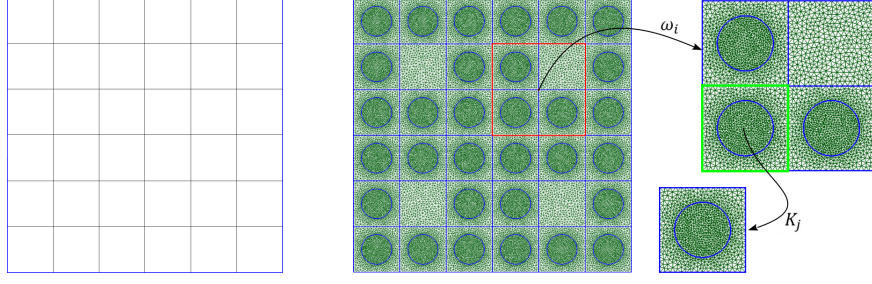


Figure 1: Coarse grid and local domain  $\omega_i$  with  $K_j$

We construct the multiscale function space

$$V_{\text{off}} = \text{span}\{y_j\}_{j=1}^N,$$

where  $N$  is the number of coarse basis functions. Each  $y_j$  is supported in local domain  $\omega_i$ .

Basis functions are designed to capture the multiscale features of the solution. Important multiscale features of the solution are incorporated into localized basis functions which contain information about the scales that are smaller (as well as larger) than the local numerical scale defined by the basis functions.

**Multiscale space.** The computation of basis functions use local spectral problems to reduce the dimension of the local problem. In order to construct conforming basis functions, we multiply eigenvectors related to dominant eigenvalues to the partition of unity functions. We use following spectral problem in  $\omega_i$

$$A\varphi^i = \lambda S\varphi^i, \quad (8)$$

where the elements of the matrices  $A = \{a_{ij}\}$  and  $S = \{s_{ij}\}$  are defined as follow

$$\begin{aligned} a_{ij} &= \int_{\omega_i} D\nabla\phi \cdot \nabla q d\mathbf{x} + \int_{\omega_i} \Sigma_r \phi q d\mathbf{x} - \int_{\omega_i} \frac{1 + \lambda\tau - \beta}{K_{eff}(1 + \lambda\tau)} \nu \Sigma_f \phi q d\mathbf{x}, \\ s_{ij} &= \int_{\omega_i} D u q d\mathbf{x}. \end{aligned} \quad (9)$$

Then, we choose eigenvectors corresponding to dominant  $M_i$  eigenvalues from (6) and use them to construct the multiscale basis functions.

**Partition of unity functions.** As partition of unity functions, we use linear functions in each domain  $\omega_i$ . Partitions of unity are calculated in the domain  $K_j$  as a linear function from  $\Gamma$  to the vertex  $A$ , and 0 is assigned to the entire segment  $\Gamma$ , and at point  $A$  is assigned the value 1. Thus, we obtain a linear function from 0 to 1 over the entire domain  $K_j$ . Partitions of unity are shown in Figure 2. Domain  $K_j$  is one element from a coarse grid.

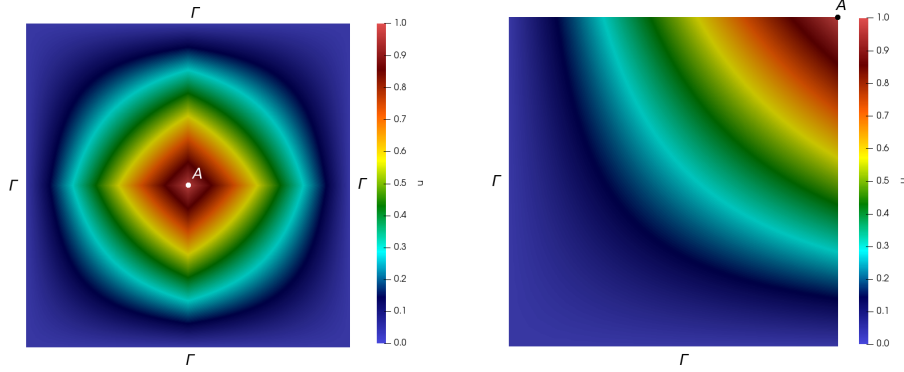


Figure 2: Partition of unity functions on the  $\omega_i$  (right) and  $K_j$  (left)

The multiscale space is defined as the span of  $y_i = \chi_i \varphi_k^i$ , where  $\chi_i$  is the usual nodal basis function for the node  $i$  (linear partition of unity functions). The number of bases can be different, the accuracy of the solution can be improved when we increase the number of bases.

**Coarse-scale approximation.** Next, we create the following matrix for each  $\omega_i$

$$R^i = [y_1, \dots, y_{M_i-1}, y_{M_i}].$$

and define the transition matrix  $R$  (transition from a fine grid to a coarse grid) to reduce the dimension of the problem

$$R = [R^1, R^2, \dots, R^{N_v}],$$

where  $N_v$  is the number of local domains  $\omega_i$ .

Then using the transition matrix  $R$  and fine grid system (5), we construct the coarse grid approximation

$$A_c \phi_c = b_c, \quad A_c = R A_f R^T \quad \text{and} \quad b_c = R b_f, \quad (10)$$

and using the coarse-scale solution  $\phi_c$ , we can reconstruct the fine grid solution

$$\phi_{ms} = R^T \phi_c.$$

#### 4. Numerical results

Let's consider the 2D test problem for small PWR reactor ( $\Omega$  — reactor core area). The geometrical model of the small PWR reactor core is presented in Fig.3. The diameter of the fuel rods is 0.82 cm, the cell width is 1.26 cm. Diffusion neutronics constants in the common notations are given in Table 1. There are two types of cassettes, with fuel 1%  $UO_2$  and 2%  $UO_2$ . The reflective boundary conditions (2) are used ( $\gamma = 0$ ). The following delayed neutrons parameters are used:  $\beta = 6.5 \cdot 10^{-3}$ ,  $\lambda = 0.08 \text{ s}^{-1}$  and  $v = 5 \cdot 10^5 \text{ cm/s}$ .

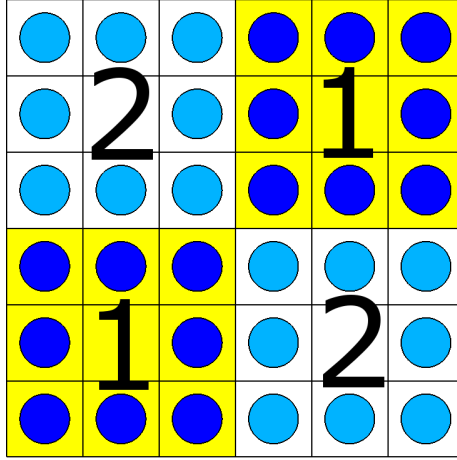


Figure 3: Geometrical model of the small PWR-2D reactor core

We define the next scenario of the process:

- The  $\lambda$ -spectral problem is solved and the solution is taken as the initial condition;
- Calculation for the non-stationary model at the time range from 0 to 0.4 sec;
- At  $t = 0.1 \text{ sec}$  and  $t = 0.3 \text{ sec}$   $\Sigma_a$  for fuel in the zone 1 changes to +2% and -3%, respectively (simulation of insertion or withdrawal of control rods).

At each time the integrated power is calculated as

$$P(t) = a \int_{\Omega} \Sigma_f \phi d\mathbf{x},$$

where  $a$  is the normalization coefficient, which corresponds to a given value of the integrated power.

The coarse grid contains 49 vertices. The fine grid contains 115891 vertices. The time step for both grids is  $\tau = 0.001$ . As an exact solution, we take the fine-grid solution. The initial value of  $K_{eff}$  is 1.183280.

Table 1: Diffusion neutronics constants for the small PWR-2D reactor core

Zone	1		2	
	coolant	fuel	coolant	fuel
$D$	0.34473872445	0.77002585054	0.31679441560	0.80236505122
$\Sigma_a$	5.3858400E-03	8.9337900E-02	6.0670900E-03	6.6279500E-02
$\Sigma_f$	0.0	5.4731800E-02	0.0	3.3377700E-02
$\nu$	0.0	2.44844861671	0.0	2.45482762443

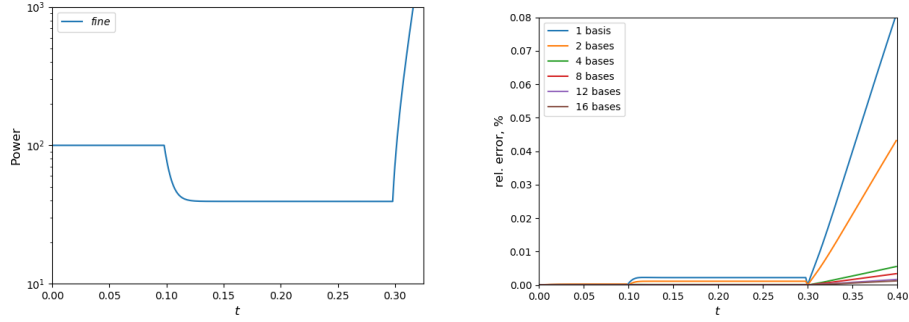


Figure 4: Integral power (the fine grid) and relative errors (%) of the multiscale solution power.

The integral power for the fine grid and relative errors of integral powers are shown in Figure 4. When using single basis, the error does not exceed 1%, and for using 4 or more bases it does not exceed 0.01%.

In Figure 5, we present relative  $L_2$  and  $H_1$  errors of the multiscale solution vs. time for different number of multiscale basis functions. The numerical results show good convergence behaviour, provided that we take sufficient number of the multiscale basis functions.

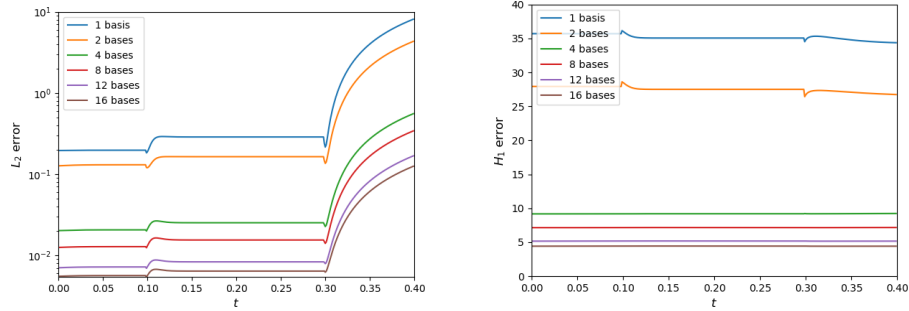


Figure 5: Relative  $L_2$  and  $H_1$  errors (%) of the multiscale solution.

In Table 2, we present relative  $L_2$  and  $H_1$  errors at final time for different

number of the multiscale basis functions. For example, when we use 8 spectral basis functions, we obtain 0.34% for  $L_2$  error and 7.18% for  $H_1$  error. Our calculations show that it is necessary to use 4 or more basis functions. In Figure 6, we present first four (of 16) multiscale basis functions in local domain  $\omega_i$ . The fine-grid solution and the multiscale solution (16 basis functions on each local domain)  $\omega_i$  are shown in Figure 7. Relative errors are 0.13% for  $L_2$  and 4.43% for  $H_1$ .

Table 2: Relative  $L_2$  and  $H_1$  errors (%) of the solution at final time.

Number of bases	Number of DOF	$L_2$ error	$H_1$ error	Calc time
1	49	8.09	34.36	0.015
2	98	4.32	26.73	0.018
4	196	0.56	9.24	0.026
8	392	0.34	7.18	0.056
12	588	0.17	5.17	0.102
16	784	0.13	4.43	0.239
fine	115891	—	—	6.816

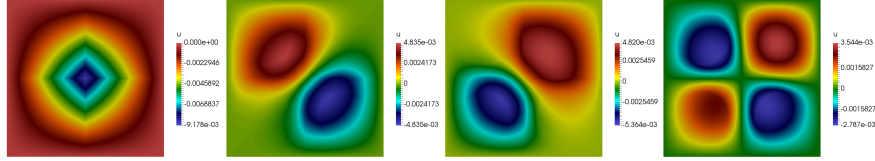


Figure 6: The first four multiscale basis functions.

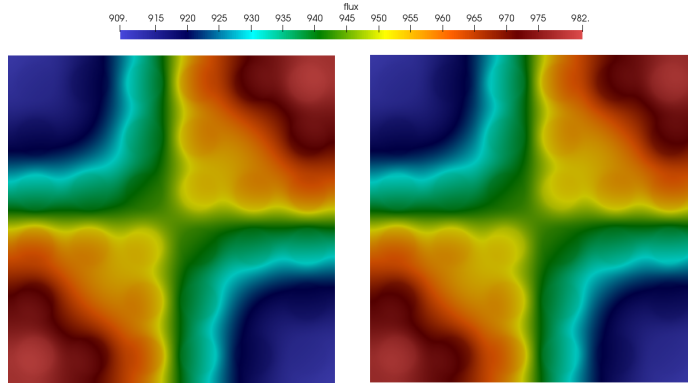


Figure 7: Fine grid and multiscale solution with 16 basis functions at final time.



## 5. Conclusions

A Generalized Multiscale Finite Element method was developed successfully for modelling neutron transport in one-group diffusion approximation. We presented an implementation of GMSFEM. We considered each step of GMSFEM algorithm. The results showed that GMSFEM performed with a good accuracy in all considered cases.

In the current work, we considered the most popular and simplest model of neutron transport equation. Computational expenses are always an issue even for modern computers. In the future, we will consider more complex models of neutron transport, such as  $SP_3$  approximation.